Orbital: The Electronic Journal of Chemistry
journal homepage: www.orbital.ufms.br
e-ISSN 1984-6428

| Vol 11 | | No. 6 | | Special Issue November 2019 |

FULL PAPER

TiO_2NT as Platform for Drug Release: The Effect of Film Wettability

Anna Paulla Simon*[a], Carlise Hannel Ferreira[a], Andressa Rodrigues[b], Janaina Soares Santos[b], Francisco Trivinho Strixino[b], Patrícia Teixeira Marques[a], Henrique Emilio Zorel Junior[a], and Mariana de Souza Sikora[a*]

[a]Chemistry Department, Universidade Tecnológica Federal do Paraná (UTFPR), Mail Box 571, 85503-390, Pato Branco, PR, Brazil.
[b]Department of Physics, Chemistry and Mathematics, UFSCar, Sorocaba, SP, Brazil.

Article history: Received: 20 September 2018; revised: 11 October 2019; accepted: 16 October 2019. Available online: 21 November 2019. DOI: http://dx.doi.org/10.17807/orbital.v11i6.1251

Abstract:

Modifications of Ti–based surface are increasingly studied to improve biological responses on the biomedical implants field. In this study, nanotubular arrays were grown from Ti_{cp} (T) and its alloy, Ti_6Al_4V (A), by potentiostatic anodization at 25 V for 90 min in ethylene glycol media containing 0.75 % w/w of NH_4F, H_2O 9% v/v and 1% v/v of Simulated Body Fluid (SBF) maintained at 10 °C (T10 and A10) and 40 °C (T40 and A40) for drug release studies. Coatings were top filled with cefazolin (1 mg) and the releasing procedure was performed in 5 mL of PBS at 37 °C, taking 0.5 mL aliquots at 1, 4, 7, 10, 15 and 30 min. The as-formed coatings were characterized by Scanning Electron Microscopy (SEM), X-rays Diffraction (XRD) and contact angle measurements. Contact angle measurements indicate that T-based nanotubular coatings are highly wettable, being ≈ 0.00° and 6.74° ± 1.96 for T10 and T40 respectively. Coatings obtained from Ti-alloy exhibits low wettability than T-based samples for both temperatures. All samples release the drug on short time intervals (4 to 10 min). The drug release rate is inversely proportional to the contact angle, considering substrate groups. Thus, a higher wettability tendency presents a higher release rate. This result shows that wettability is an important parameter to be considered in the design of Ti-based biomaterials.

Keywords: drug release; potentiostatic anodization; Ti-based biomaterials; wettability.

1. Introduction

Titanium-based materials are one of the most studied compounds in the materials science field. The reason for this is its diverse molecular combining ability, resulting in totally different chemical, mechanical and electrical properties [1].

One of the examples of the use of these properties is in biomaterials. The choice of a biomaterial follows specific criterions, being governed by proprieties that include biocompatibility, corrosion resistance, controlled degradability, elastic modulus and others [2]. In this sense, Ti-based biomaterials are often preferred over other materials due to the combination of mechanical and chemical resistance, especially on bone-related applications (dental and orthopedic applications) [3].

The main metals used in orthopedic applications are F67 commercially pure titanium and F136 titanium–aluminum–vanadium alloy (Ti_6Al_4V) [3, 4]. Some literature about metallic titanium biomaterials shows an absence of blood compatibility and bioactivity [5]. But, nowadays, nanotechnology presents an opportunity for surface modification of metals by creating oxide coatings designed for better performance of these existing materials, like biomedical applications [6, 7]. The functionalization of these metal substrates can be achieved by various techniques, in which it stands out anodization process [8].

By controlling the variables, anodic films can

*Corresponding author. E-mail: anna17simon@gmail.com

present nanoarchitectures that modify its interaction with the human body, by mimetizing or tailoring surface properties. This modification aggregates etch protection, anti-corrosion and even specific areas that induce deposition of species of biological interest and for drug loading [9]. Antibiotic loading may be the key to reducing high rejection rate increases triggered by bacteria cell proliferation and biofilm formation [10].

In this sense, this study aimed to investigate the influence of the synthesis parameters on the physical properties of TiO_2 nanotubes applied to the biomedical field. Due to the high surface area of coatings, their applicability as drug delivery devices has also been investigated. The objective is to contribute to the study of the use of these materials on the restoration of human mechanical and biological functions.

2. Results and Discussion

Fig. 1 shows the current transients (Current Density - CD versus time) recorded during T and A anodization at a constant voltage of 25 V, maintained at 10 and 40 °C. It can be seen, for all processes, that CD decreases exponentially to a minimum (MCD) in the first few seconds (Stage II), related to the formation of a compact oxide [8]. After this point, CD increases to a maximum (MACD), explained by the non-uniform attack of the barrier oxide by fluoride ions that originates the nanopores. After this stage, CD enters into a quasi-steady stage, wherein the rates of oxide formation and dissolution are constant [11].

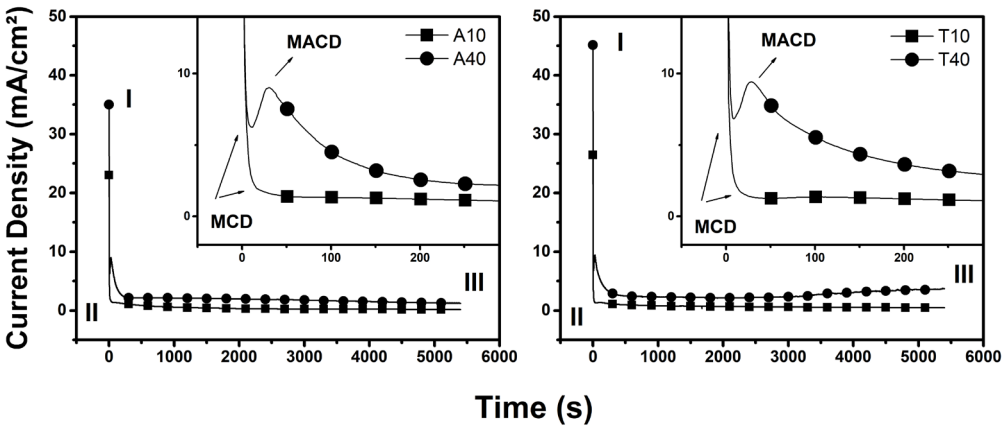

Figure 1. Current Density (mA/cm²) versus Time (s) curves of all samples anodized at 10 and 40 °C.

The effect of synthesis temperature can be visualized by a change of CD in stage II, of MCD and MACD. At 10 °C anodization, the exponential CD decrease leads to constant values at 50 seconds, wherein no CD peak is seen. When the temperature is increased to 40 °C, the CD decrease is followed by a significant change in slope to MACD, creating a CD peak. Regarding the formed slope, it could be suggested that the variation of differential dissolution rates of the oxide layer, since the alteration of the temperature changes the viscous, and consequently the attack of fluoride ions, as highlighted in [12]. This effect of the temperature on morphology can be demonstrated in Fig. 2a.

Micrographs analysis (Fig. 2a) reveals the formation of perpendicular NTs arrays homogeneously distributed in metallic substrates. Coatings synthesized at different temperatures present slight changes in morphology: lower temperatures induce the growth of more organized nanostructures while in high temperatures there is the growth of less organized structures, in which the union of the superior portion of the nanopores can be visualized. Also, there is an effect in inner pore diameter (Di), extracted from SEM by Image J treatment [13], presented in Table 1. Contrasting the contact angle data between the substrates, there is an increase in Di as a function of electrolyte temperature, which has induced higher wettability behavior (Fig. 2a), as presented in [14].

The wettability behavior of surfaces can be explained as a couple of morphology effects and

chemical constitution. In this sense, the greater uniformity of the surface is directly related to a decrease of the wettability, phenomena expected as a function of surface roughness discussed in [15]. The values extracted by contact angles (Fig. 2a) are presented in Table 1 (column 1), wherein the values obtained for samples synthesized at 10 °C are lower than those synthesized at 40 °C.

The as-prepared nanotubes arrays were found to be composed of amorphous titanium Dioxide, in which titanium substrate X-ray pattern diffraction could be observed (Fig. 2b), typical for anodic oxide films grown by similar anodization process [16].

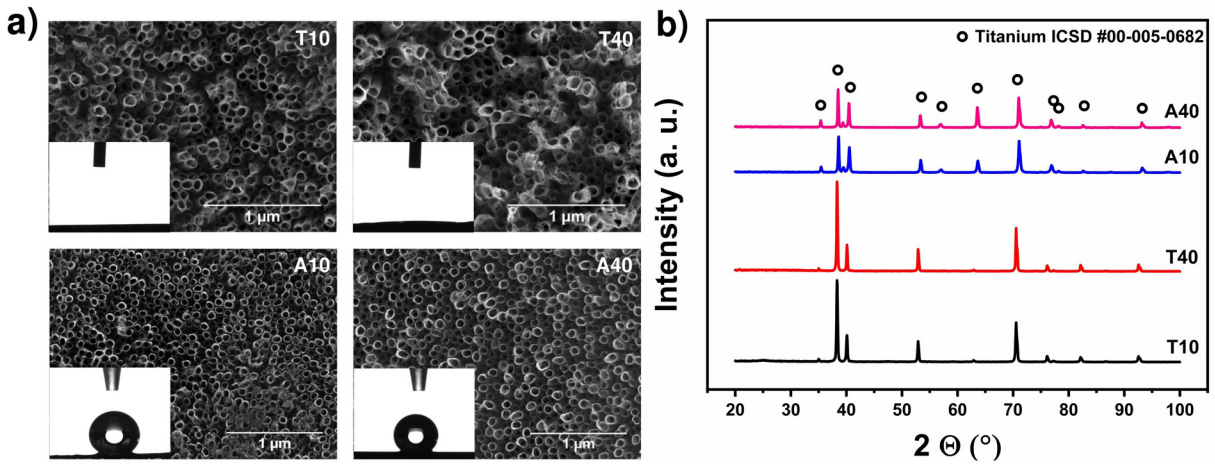

Figure 2. a) FE-SEM images with contact angles (inset) and b) X-rays patterns of as-prepared TiO_2NT anodized at 10 and 40 °C.

Table 1. Inner pore diameter (Di) and **c**ontact angle values for TiO_2NT samples anodized at 10 and 40 °C and its effect on the time of total mass release parameters extracted from Fig. 3.

	Inner pore diameter (nm)	Contact angle (°)	Time for total mass release (min)
T10	61.96±1.18^{c}	≈ 0.00^{d*}	4.00±0.00^{b}
T40	78.28±1.25^{a}	6.74±1.96^{c}	8.50±1.50^{a}
A10	58.46±0.14^{c}	151.05±0.55^{b}	4.00±0.00^{b}
A40	72.22±0.75^{b}	164.60±0.90^{a}	7.00±0.00^{a,b}

* Data are expressed as means ± standard deviations.
* Values that share the same letter does not present statistical significant difference.

According to Yasuda and K.; Schmuki and LeCleire [17, 18], the differential diffusion and attack of fluoride ions in the oxide layer as credited as the main factor for NTs growth. As highlighted before, the increase in temperature has an impact on electrolyte viscosity, increasing oxide dissolution rates [12]. According to the definition of ionic mobility (u) under a constant electric field (eq. (1)), it could be seen that an inverse relationship between the ion migration rate and the viscosity of the medium, in which, z_e, η and a are respectively the charges of the ion, electric field module, viscosity, and ionic radius:

$$u = z_e E / 6\Pi\eta a \quad (1)$$

The increase in electrolyte temperatures reduces the viscosity of electrolyte which is related to an increase in ionic migration. Thus, from increasing electrolyte temperature from 10 to 40 °C, the mass transport increases and, consequently, the dissolution rate rises. For this reason, the pore diameter also increases more than 10 nm when anodization is performed at 40 °C.

The presence of these nanostructures can significantly increase the surface area of the material [19] and in biomedical applications, enhance the interaction with surrounding fluids. Fig. 3 shows the accumulative mass release of sodium cefazolin from titanium nanotubes arrays with different wettability behavior. The plot of mass release shows that released mass increases with increasing immersion time, as expected. The total mass time is presented in Table 1.

Drug release pattern, presented in Fig. 3 and Table 1, shows that A10 and T10 samples

release the total mass loaded in 4 minutes. A40 and T40 samples released all mass in 8.5 and 10 minutes, respectively. So, relatively, the slow release rate of sodium cefazolin was provided by samples anodized at 40 °C. This found leads to the following observation: more hydrophobic the surface, the lower the dissolution and CS release due to the decrease of the coating interaction with water.

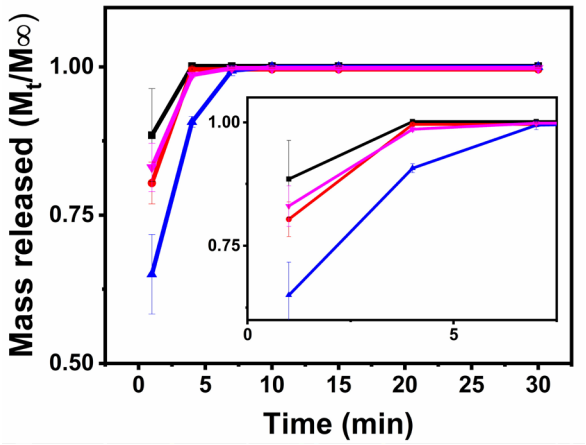

Figure 3. Cumulative mass release plot of sodium cefazolin by TiO_2NT samples anodized at 10 and 40 °C.

The literature indicates that mass transfer of drug-loaded nanotubular coatings is described by diffusional mechanism [22], being influenced by drug's molecular size, drug-implant interaction, tube dimensions and others [19,22]. These properties can induce different profiles of drug release, such as burst or prolonged release. Burst release profile comprises free diffusion of drug leaded throw time, wherein high quantities of the drug are released in earlier times after drug administration. For local drug delivery systems, this kind of mechanism must be avoided to minimize, for example, the toxic effects of high doses [23]. As the interaction of the drug with the surface increases or when introduced diffusion limiters, like polymers, the release becomes slower, decreasing the angular coefficient of the first minutes of the curve, decreasing toxic effects.

Comparing all samples, the T10 and A10 coatings show lower contact angle values compared to T40 and A40, respectively. For these samples, a shorter release time was observed. This result can be explained by the increased wettability of the material, *i. e.* a greater interaction of the coating with water, inducing lower drug diffusion rates.

3. Material and Methods

3.1 TiO_2NT coatings preparation and characterization

Nanotubular arrays were grown from 1200 mesh polished Ticp (T) and its alloy Ti_6Al_4V (A), by potentiostatic anodization at 25 V for 90 minutes in a two-electrode cell, using a pair of platinum sheet as counter electrode. The electrolyte was constituted by 0.75% w/w of NH_4F, H_2O 9% v/v, Simulated Body Fluid (SBF) 1% v/v in ethylene glycol maintained at 10 °C (T10 and A10) and 40 °C (T40 and A40) by a thermostatic bath. After anodized, the samples were washed with water and dried at room temperature. All experimental conditions are shown in Table 2.

As-prepared TiNTs was characterized by a field-emission scanning electron microscope (FEG-SEM Zeiss Supra 35), followed by pore inner diameters (Dp) analysis using ImageJ software [13]. Structural analysis was carried out in a Higaku 600 Benchtop X-ray Diffraction (XRD), Cukα (0.15418 nm), operating at 40 kV and 15 mA from 20 to 100 (2 Theta) at a rate of 5 °/min. Wettability analysis was performed in a hamé-hart Goniometer/Tensiometer, Model 250, measured 60 seconds after placing droplet on TiO_2 surface, to soften water absorption by the nanostructures [24].

Table 2. 2^2 factorial design matrix showing the synthesis conditions of TiO_2NT coatings.

	Substrate	Temperature (°C)
T10	Titanium cp	10
T40	Titanium cp	40
A10	Titanium alloy	10
A40	Titanium alloy	40

3.2 Drug Loading and Delivery Assay

Cefazolin sodium (CS), supplied by Abl - Antibioticos do Brasil, was loaded into TiO_2NT arrays via top filling physical adsorption by Feng, et al. adapted methodology [25]. A 10 mg/mL water solution of CS was prepared in water and 10 µL of CS solution was pipetted onto the anodic surface, being gently spread to ensure all

anodic area coverage, dried at 25 °C in an incubator with air circulation. After drying, this process was repeated 5 times on each face, loading the nanostructures with 1 mg.

Drug delivery assay was performed by immersion in 5mL of PBS maintained at 37 °C with a thermostatic bath, according to the adapted methodology of Losic, et al. [26]. Aliquots of 0.5 mL were taken in 1, 4, 7, 10, 15 and 30 minutes, being replaced with 0.5 mL of fresh PBS to maintain sink condition [27]. Drug released measurements were investigated using ultraviolet–visible spectroscopy (Shimadzu, UV-1800) at 243 nm, diluting the samples in PBS. The amount of drug released in time was determined with CS calibration curve.

3.4 Statistical analysis

Statistical significance was analyzed by Single-factor analysis of variance (ANOVA) using a confidence level of 95%, where the influence of the experimental conditions on drug delivery test was observed. The results data were expressed as the mean ± standard deviation (SD), denoted by overwritten letters. Values that present the same letter are not significantly different.

4. Conclusions

The results show that TiO_2NT films can be formed at 10 and 40 °C and the temperature present an important role in coating wettability. It was observed that coatings anodized at 40 °C presents inner pore diameter more than 10 nm higher than those prepared at 10 °C. As wettability can be related to pore diameter, TiO_2NT coating prepared at 10 °C from titanium presents a higher hydrophilic behavior than the oxide prepared at 40 °C. The same behavior was observed in alloy-based samples. The analysis of drug release assay reveals that lower wettability behavior favored slower dissolution and release rates of CS. This result can be related to an increase in drug-surface interaction and at the same time, a decrease in water interaction. In summary, wettability reveals to be an important parameter to be considered in the design of Ti-based biomaterials, especially if the purpose of the coating is to serve as a device for drug release.

Acknowledgments

The authors are grateful to Abl - Antibioticos do Brasil for CS supply, to LIEC-UFSCar and Analysis Center of UTFPR-PB. This work was supported by UTFPR [PAPCDT 06/2016 and 07/2017]. This study was financed in part by the Coordenação de Aperfeiçoamento de Pessoal de Nível Superior - Brasil (CAPES) - Finance Code 001.

References and Notes

[1] Roy, P.; Berger, S.; Schmuki, P. *Angew. Chem., Int. Ed.* **2011**, *50*, 2904. [Crossref]

[2] Mahapatro, A. *Mater. Sci. Eng., C* **2015**, *55*, 227. [Crossref]

[3] Kohn, D. H. *Curr. Opin. Solid State Mater. Sci.* **1998**, *3*, 309. [Crossref]

[4] Castner, D. G.; Ratner, B. D. *Biomedical surface science:* Foundations to frontiers 2002.

[5] Rimondini, L.; Bianchi, C. L.; Vernè, E. *Surface Tailoring of Inorganic Materials for Biomedical Applications* Bentham Science Publishers: Naples, 2012.

[6] Lemons, J. E. *Journal of Oral Implantology* **2004**, *30*, 318. [Crossref]

[7] Sperling, C.; Schweiss, R. B.; Streller, U.; Werner, C. *Biomaterials* **2005**, *26*, 6547. [Crossref]

[8] Regonini, D.; Bowen, C. R.; Jaroenworaluck, A.; Stevens, R. *Mater. Sci. Eng., R* **2013**, *74*, 377. [Crossref]

[9] Gulati, K.; Aw, M. S.; Losic, D. *Nanoscale Res. Lett.* **2011**, *6*, 1. [Crossref]

[10] Wei, D.; Zhou, R.; Cheng, S.; Feng, W.; Li, B.; Wang, Y.; Jia, D.; Zhou, Y.; Guo, H. *Mater. Sci. Eng., C* **2013**, *33*, 4118. [Crossref]

[11] Beranek, R.; Tsuchiya, H.; Sugishima, T.; Macak, J. M.; Taveira, L.; Fujimoto, S.; Kisch, H.; Schmuki, P. *Appl. Phys. Lett.* **2005**, *87*, 1. [Crossref]

[12] Macak, J. M.; Schmuki, P. *Electrochim. Acta* **2006**, *52*, 1258. [Crossref]

[13] Schneider, C. A.; Rasband, W. S.; Eliceiri, K. W. *Instrumentation, C. Nature Methods* **2012**, *9*, 671.

[14] Liu, G.; Du, K.; Wang, K. *Appl. Surf. Sci.* **2016**, *388*, 313. [Crossref]

[15] Rupp, F.; Gittens, R. A.; Scheideler, L.; Marmur, A.; Boyan, B. D.; Schwartz, Z.; Geis-gerstorfer, J. *Acta Biomater.* **2014**, *10*, 2894. [Crossref]

[16] Prida, V. M.; Manova, E.; Vega, V.; Hernandez-Velez, M.; Aranda, P.; Pirota, K. R.; Vázquez, M.; Ruiz-Hitzky, E. *J. Magn. Magn. Mater.* **2007**, *316*, 110. [Crossref]

[17] Yasuda, K.; Schmuki, P. *Electrochim. Acta* **2007**, *52*, 4053. [Crossref]

[18] LeClere, D. J.; Velota, A.; Skeldon, P.; Thompson, G. E.; Berger, S.; Kunze, J.; Schmuki, P.; Habazaki, H.; Nagata, S. *J. Electrochem. Soc.* **2008**, *155*, C487. [Crossref]

[19] Macak, J. M.; Tsuchiya, H.; Ghicov, A.; Yasuda, K.; Hahn, R.; Bauer, S.; Schmuki, P. *Curr. Opin. Solid State Mater. Sci.* **2007**, *11*, 3. [Crossref]

[20] Shin, D. H.; Shokuhfar, T.; Choi, C. K.; Lee, S. H.; Friedrich, C. *Nanotechnology* **2011**, 22. [Crossref]

[21] Liu, K.; Cao, M.; Fujishima, A.; Jiang, L. *Chem. Rev.* **2014**, *114*, 10044. [Crossref]

[22] Sinn Aw, M.; Kurian, M.; Losic, D. *Biomater. Sci.* **2013**, *2*, 10. [Crossref]

[23] Huang, X.; Brazel, C. S. *J. Controlled Release* **2001**, *73*, 121. [Crossref]

[24] Sabonis, V.; Naujokaitis, A.; Arlauskas, K. *J. Laser Micro/Nanoeng.* **2015**, *10*, 24. [Crossref]

[25] Feng, W.; Geng, Z.; Li, Z.; Cui, Z.; Zhu, S.; Liang, Y.; Liu, Y.; Wang, R.; Yang, X. *Mater. Sci. Eng., C* **2016**, *62*, 105. [Crossref]

[26] Gulati, K.; Kogawa, M.; Prideaux, M.; Findlay, D. M.; Atkins, G. J.; Losic, D. *Mater. Sci. Eng., C* **2016**, *69*, 831. [Crossref]

[27] Wachol-Drewek, Z.; Pfeiffer, M.; Scholl, E. *Biomaterials* **1996**, *17*, 1733. [Crossref]